Wall teichoic acid substitution with glucose governs phage susceptibility of *Staphylococcus epidermidis*

Christian Beck[a,b,c], Janes Krusche[a,b,c], Anna Notaro[d], Axel Walter[a,e], Lara Kränkel[a,b,c], Anneli Vollert[f], Regine Stemmler[a,b,c], Johannes Wittmann[g], Martin Schaller[f], Christoph Slavetinsky[a,b,c,h], Christoph Mayer[a,e], Cristina De Castro[i], Andreas Peschel[a,b,c,#]

[a]Cluster of Excellence "Controlling Microbes to Fight Infections (CMFI)", University of Tübingen, Tübingen, Germany

[b]Interfaculty Institute of Microbiology and Infection Medicine Tübingen, Infection Biology, University of Tübingen, Tübingen, Germany

[c]German Centre for Infection Research (DZIF), Partner Site Tübingen, Tübingen, Germany

[d]Department of Agricultural Sciences, University of Naples, Naples, Italy

[e]Interfaculty Institute of Microbiology and Infection Medicine Tübingen, Organismic Interactions/Glycobiology, University of Tübingen, Tübingen, Germany

[f]Electron-Microscopy, Department of Dermatology, University Hospital Tübingen, Tübingen, Germany

[g]Leibniz Institute, DSMZ-German Collection of Microorganisms and Cell Cultures, Braunschweig, Germany

[h]Pediatric Surgery and Urology, University Children´s Hospital Tübingen, University of Tübingen, Germany

[i]Department of Chemical Sciences, University of Naples, Naples, Italy

[#]Correspondence to Andreas Peschel (andreas.peschel@uni-tuebingen.de)

Abstract: 301 words

Article: 4989 words

Abstract

The species- and clone-specific susceptibility of *Staphylococcus* cells for bacteriophages is governed by the structures and glycosylation patterns of wall teichoic acid (WTA) glycopolymers. The glycocodes of phage-WTA interaction in the opportunistic pathogen *Staphylococcus epidermidis* and in other coagulase-negative staphylococci (CoNS) have remained unknown. We report a new *S. epidermidis* WTA glycosyltransferase TagE whose deletion confers resistance to siphoviruses such as ΦE72 but enables binding of otherwise unbound podoviruses. *S. epidermidis* glycerolphosphate WTA was found to be modified with glucose in a *tagE*-dependent manner. TagE is encoded together with the enzymes PgcA and GtaB providing uridine diphosphate-activated glucose. ΦE72 transduced several other CoNS species encoding TagE homologs suggesting that WTA glycosylation via TagE is a frequent trait among CoNS that permits inter-species horizontal gene transfer. Our study unravels a crucial mechanism of phage-*Staphylococcus* interaction and of horizontal gene transfer and it will help in the design of anti-staphylococcal phage therapies.

Importance

Phages are highly specific for certain bacterial hosts, and some can transduce DNA even across species boundaries. How phages recognize cognate host cells remains incompletely understood. Phages infecting members of the genus *Staphylococcus* bind to wall teichoic acid (WTA) glycopolymers with highly variable structures and glycosylation patterns. How WTA is glycosylated in the opportunistic pathogen *Staphylococcus epidermidis* and in other coagulase-negative *Staphylococcus* (CoNS) species has remained unknown. We describe that *S. epidermidis* glycosylates its WTA backbone with glucose and we identify a cluster of three genes, responsible for glucose activation and transfer to WTA. Their inactivation strongly alters phage susceptibility patterns, yielding resistance to siphoviruses but susceptibility to podoviruses. Many different CoNS species with related glycosylation genes can exchange DNA via siphovirus ΦE72 suggesting that glucose-modified WTA is crucial for interspecies horizontal gene transfer. Our finding will help to develop antibacterial phage therapies and unravel routes of genetic exchange.

Introduction

Staphylococcus epidermidis is one of the most abundant colonizers of mammalian skin and of nasal epithelia [1, 2]. Some nosocomial *S. epidermidis* clones also cause invasive infections, in particular biofilm-associated infections on catheters or artificial implants such as hip and knee joints or heart valves [3, 4]. Although *S. epidermidis* is not an as aggressive pathogen as *Staphylococcus aureus*, biofilm-associated infections are difficult to treat and cause a high burden of morbidity and costs for health care systems. Many *S. epidermidis* clones are resistant to beta-lactams and other antibiotics such as linezolid, which further complicates the treatment of *S. epidermidis* infections [1].

The major invasive *S. epidermidis* clones seem to pursue two different virulence strategies. The MLST type 2 (ST2) strains produce particularly strong biofilms [3, 5]. In contrast, ST10, ST23, and ST87 clones are only weak biofilm formers, but they express an additional surface molecule that alters their host interaction capacities and leads to a shift from commensal to pathogen behavior [6]. Surface properties and host interaction of staphylococci are governed not only by surface proteins but also by cell-wall anchored glycopolymers composed of alditolphosphate repeating units called wall teichoic acids (WTA) [7, 8]. The WTA polymers of *S. epidermidis* and other coagulase-negative *Staphylococcus* (CoNS) species have remained a neglected field of research despite their potentially critical role for host colonization and infection. Most *S. epidermidis* clones seem to express WTA composed of glycerolphosphate (GroP) repeating units [9]. A recent study has shown that ST10, ST23, and ST87 strains express an additional *S. aureus*-type WTA composed of ribitolphosphate (RboP) repeating units, which shapes their interaction with human epithelial and endothelial cells [6].

WTA is also crucial for binding of virtually all known *Staphylococcus* phages, which use differences in WTA structure to recognize their cognate host species [10]. Phages of the Sipho- and podovirus groups often not only discriminate between different WTA backbones but also between different types of backbone glycosylation. Most Firmicutes link D-alanine esters and sugar residues to GroP or RboP repeating units [7, 8]. Variation in glycosylation for instance by N-acetylglucosamine (GlcNAc) in alpha or beta configuration or N-acetylgalactosamine (GalNAc) has been found to govern the susceptibility patterns of *S. aureus* strains for different phages [11-14]. The group of broad-host range myoviruses, however, requires WTA for binding but does not discriminate between RboP and GroP WTA and does not require WTA glycosylation [15-17].

WTA-phage interaction is of importance for phage-therapeutic strategies, which have gained increasing attention recently [3, 18]. Moreover, they are critical for inter-species horizontal gene transfer via transducing bacteriophages [19]. Such transduction events have led to the transfer of resistance and virulence genes into the genomes of *S. aureus* and other species, thereby allowing, for

instance, evolution of methicillin-resistant *S. epidermidis* (MRSE) and methicillin-resistant *S. aureus* (MRSA) [20, 21]. Despite the critical role of WTA in these processes, the biosynthesis, composition, and glycosylation of the canonical *S. epidermidis* WTA has not been studied.

Here we demonstrate, that *S. epidermidis* strain 1457 glycosylates its GroP-WTA with glucose and we identify the WTA glucosyltransferase gene *tagE*. *S. epidermidis tagE* mutants showed complex changes in phage susceptibility patterns including both, the loss, and the acquisition of susceptibility to certain phages, some of which we found to be capable of transducing plasmid DNA between different CoNS species.

Results

1. Disruption of a putative glycosyl transferase gene cluster confers resistance to phage ΦE72

Several new phages with the capacity to infect *S. epidermidis* have been reported recently [22, 23]. Some of them have the capacity to transduce DNA between different *S. epidermidis* lineages, raising the question, which bacterial target structures are recognized by the phages' binding proteins, and how universal these target structures may be among different clones of *S. epidermidis* and other CoNS. As most *S. aureus* phages recognize the sugar modifications of WTA [11-13, 24], it was tempting to speculate that glycosylated GroP-WTA is also required for binding of *S. epidermidis* phages. However, the enzymes responsible for WTA glycosylation in *S. epidermidis* have remained unknown and it has also remained elusive, which glycosylation patterns can be found on *S. epidermidis* GroP-WTA. To elucidate the WTA glycosylation pathways of *S. epidermidis* and explore its impact on phage interaction we set out to identify and inactivate the responsible enzyme genes.

A library of transposon mutants of *S. epidermidis* 1457 was created using a xylose-inducible Himar1 transposase [25] and incubated with phage ΦE72, which is known to infect and multiply in strain 1457 [22]. Two mutants, which were resistant to ΦE72 were identified and found to have the transposon integrated in two adjacent genes of unknown function (Fig. 1a; Fig. 2a, d). The two genes were not in the vicinity of other WTA-biosynthesis related genes, but their gene products shared similarity with glycosylation-related enzymes. The gene B4U56_RS02220 product was 46% similar to TagE of *Bacillus subtilis*, which glycosylates GroP-WTA with glucose residues [26] and 48% similar to TarM of *S. aureus,* which glycosylates RboP-WTA with GlcNAc (Fig. 1b) [27]. The adjacent gene B4U56_RS02215 encodes a protein with 59% similarity to the phosphoglucomutase PgcA of *B. subtilis*, which isomerizes glucose-6-phosphate to yield glucose-1-phosphate [28]. In addition, the product of gene B4U56_RS02210, next to *pgcA,* was 85% similar to the GtaB enzyme of *B. subtilis* generating UDP-glucose from glucose-1-phosphate and UTP [29]. Both, PgcA and GtaB are required for glycosylation of GroP-WTA with glucose

via TagE in *B. subtilis* [30], although the two genes are not encoded together with *tagE* in *B. subtilis* [31, 32]. We assumed that the three enzymes might cooperate in *S. epidermidis* to activate and attach glucose to GroP-WTA.

2. *S. epidermidis* TagE is responsible for glucose addition to GroP-WTA

The three *S. epidermidis* genes were renamed according to the corresponding *B. subtilis* genes *tagE*, *gtaB*, and *pgcA.* All three genes were inactivated by targeted deletion to confirm their roles in phage susceptibility. The three mutants were as resistant to ΦE72 infection as the transposon mutants, and complementation of the *tagE* mutant with a plasmid-encoded copy of the gene locus restored wild-type level ΦE72 susceptibility (Fig. 2 c,f). The various transposon and targeted deletion mutants were approximately 3-fold less susceptible to ΦE72 infection, but were not completely resistant, suggesting that the phage may have additional, albeit less effective ways to interact with *S. epidermidis* 1457. In a similar way, and even more pronounced, the mutants had retained only limited capacities to bind ΦE72 particles in liquid media (Fig. 2 d-f; Fig S1).

WTA isolated from 1457 wild type (WT) contained substantial amounts of glucose when analyzed by an enzymatic glucose assay indicating that ca. 50% of the GroP-WTA repeating units are modified with glucose (Fig. 3a). In contrast, none of the WTA samples of any of the *tagE*, *gtaB*, or *pgcA* mutants was found to contain glucose. High-performance liquid chromatography coupled to a mass spectrometry detector (HPLC-MS) and nuclear magnetic resonance (NMR) spectroscopy confirmed the presence of glucose-substituted GroP repeating units in the wild type and the absence of glucose in the mutants (Fig. 3b,c; Fig. S2). These findings reflect earlier reports on the presence of glucose on *S. epidermidis* GroP-WTA [9] and they confirm that the PgcA-GtaB-TagE pathway is required for GroP-WTA glycosylation with glucose. NMR analysis indicated that the glucose units are α configured at the anomeric center and attached to the C2-position of GroP. About 15% of the glucose residues are modified with D-alanine at the O6-position of glucose (Fig. 3c; NMR extended description). The α-configuration is reminiscent of the configuration of GlcNAc on RboP-WTA introduced by the TagE-related TarM in *S. aureus* [27].

The absence of glucose on GroP-WTA in the Δ*tagE* mutant did not alter biofilm formation by *S. epidermidis* 1457 (Fig. S3). Moreover, no differences in growth kinetics (Fig. S1), cell wall thickness, or cell shape (Fig. S4) were observed in the mutants, indicating that the absence of glucose on GroP-WTA has no major impact on overall cellular properties of the *S. epidermidis* surface.

UDP-glucose generated by PgcA and GtaB is also required for biosynthesis of the glycolipid diglucosyldiacylglycerol (DGlcDAG), which serves as anchor structure for lipoteichoic acid (LTA)

polymers in *B. subtilis* and many other Firmicutes (Fig 4a) [33-35]. However, DGlcDAG is not essential for LTA biosynthesis because mutants lacking the glycolipids still produce LTA attached to phosphatidylglycerol lipids [35, 36]. The *S. epidermidis pgcA* and *gtaB* mutants, but not the *tagE* mutant, also lacked DGlcDAG, which was present in the parental strain (Fig. 4b), indicating that DGlcDAG is synthesized in *S. epidermidis* by the same pathway as in *B. subtilis* and *S. aureus*.

3. Lack of WTA glucose impairs binding of known *S. epidermidis* siphoviruses but promotes binding of podoviruses

Several other phages in addition to ΦE72 were analyzed for an impact of GroP-WTA glucose modification on phage binding and infection. The ΦE72-related siphoviruses Φ456, Φ459, and Φ27, which are known to bind to *S. epidermidis* 1457 [22], showed reduced binding to the *pgcA, gtaB*, and *tagE* mutants compared to the wild type but the reduction was less pronounced as for ΦE72 (Fig. 5a,f). Φ459 was equally reduced in its capacities to propagate in the mutants as ΦE72 (Fig. 5b). Despite their capacity to bind *S. epidermidis* 1457, Φ27 and Φ456 did not form clear plaques on wild-type or mutant strains. Two recently isolated myoviruses of the genus sepunavirus, ΦBE04 and ΦBE06 [37], showed no reduction in their ability to bind and infect the mutants, suggesting that these myoviruses are not dependent on glucose-modified GroP-WTA (Fig. 5d,e). This behavior resembles the lacking impact of WTA glycosylation on myovirus ΦK infection of *S. aureus* [13].

Several other phages, which bind *S. epidermidis* 1457 but cannot replicate in this strain, behaved differently. Siphovirus Φ187, which is only distantly related to ΦE72 and requires GroP-WTA modified with GalNAc for infection of target cells [24], still bound efficiently to the GroP-WTA glucose-deficient mutants (Fig. 5a), indicating that the GroP-WTA glucose modifications are not necessary for Φ187 binding. Φ187 even showed higher plasmid transduction efficiency in the absence of GroP-WTA glucose residues (Fig. 6a). Furthermore, the podoviruses ΦUKE3, ΦSpree, and ΦBE03 [37] exhibited strongly increased binding to the *pgcA, gtaB,* and *tagE* mutants compared to the wild type (Fig. 5 c,f), indicating that these phages are attenuated for binding in the presence of glucose residues on GroP-WTA. Thus, the GroP-WTA glucose residues are important for most of the known *S. epidermidis* phages albeit in quite different ways, depending on the individual phage.

4. The presence of *tagE* in the genomes of CoNS species corresponds to the capacity of ΦE72 to transduce these species

The *tagE* gene was found in virtually all available *S. epidermidis* genomes suggesting that the substitution of GroP-WTA with glucose is a general trait in *S. epidermidis*. Accordingly, ΦE72 bound well to the tested *S. epidermidis* strains from at least two different sequence types (ST86, ST32) with

one exception (Fig. 6b). Notably, ΦE72 did not bind to *S. epidermidis* E73 (ST23), which produces RboP-WTA in addition to GroP-WTA [6]. However, a E73 *tarIJLM2* mutant lacking RboP-WTA was effectively bound by ΦE72 indicating that the additional RboP-WTA shields the surface of *S. epidermidis* in a way that precludes binding of the phage.

GroP-WTA has been reported in several other CoNS species. The nature of the sugar modifications in these species has remained largely unknown, but several CoNS have been reported to contain either glucose, GlcNAc or GalNAc attached to WTA [9]. We succeeded in transducing many different CoNS species via ΦE72 with either the staphylococcal shuttle vector pBASE or the green-fluorescent protein-expressing plasmid pC183-S3 GFP. Some of the available CoNS genomes were found to encode TagE homologs albeit with different degrees of sequence conservation, ranging from 43% to 83% similarity (Table 1). Those species with TagE similarities above 67% could be transduced by ΦE72, while those with less conserved TagE homologs did not take up DNA from ΦE72 (Fig. 6c), suggesting that only CoNS with highly conserved versions of TagE may glycosylate their GroP-WTA in a similar way as in *S. epidermidis* while the others may glycosylate either other WTA backbone types or may transfer other sugars. Among the tested species, *Staphylococcus pasteuri*, *Staphylococcus lugdunensis*, *Staphylococcus cohnii*, *Staphylococcus caprae*, *Staphylococcus schleiferi*, *Staphylococcus carnosus*, *Staphylococcus simulans,* and *Staphylococcus warneri* strains were transducible with ΦE72. Isolates of two of these species*, Staphylococcus cohnii* and *Staphylococcus warneri,* have indeed previously been described to produce GroP-WTA, which is modified with glucose [9]. In contrast to the varying degrees of conservation of *tagE*, the *pgcA* and *gtaB* genes are present in virtually all *Staphylococcus* genomes with high sequence similarity, including *S. aureus*, probably because UDP-glucose is required in all these species for DGlcDAG glycolipid synthesis [36]. Among the strains that encode highly conserved TagE homologues, *tagE* was encoded in the vicinity of both *pgcA* and *gtaB* only in *S. pasteuri* and *S. lugdunensis,* in addition to *S. epidermidis* (Table 1). Thus, phage ΦE72 represents a helpful tool for studying WTA properties and an attractive vehicle for interspecies transduction of DNA among members of the genus *Staphylococcus*.

Discussion

WTA structures are known to be highly diverse among Firmicutes, often with species- or even clone-specific composition [7, 38]. Most *S. epidermidis* produce a WTA type that is entirely different from that of *S. aureus* with a GroP rather than a RboP backbone. This study shows that *S. epidermidis* uses a GroP backbone with unmodified or with alanylated glucose. It remains unclear why *S. epidermidis* and *S. aureus* have developed such entirely different WTA types. The different structures may limit the

number of bacteriophages that can infect and harm either one or both species. However, ΦK, one the most lytic bacteriophages, can lyse *Staphylococcus* cells irrespective of the WTA backbone structure and a recent study has demonstrated that several *Staphylococcus* phages can infect both, *S. aureus* and *S. epidermidis* [39]. The differences in WTA may limit infections and concomitant lysogenization or transduction events by specific members of the siphovirus group, which depend much more on a specific WTA backbone and glycosylation type than myoviruses. Notably, the presence of glucose on GroP-WTA prevented adsorption to *S. epidermidis* by all tested podoviruses (ΦUKE3, ΦSpree, and ΦBE03). The number of available *S. epidermidis*-targeting phages is still very limited, which impedes more extensive studies on the susceptibility of *S. epidermidis* wild-type and WTA mutant strains for different phage types. Discovery programs for identification of new phages that can infect *S. epidermidis* will help to clarify these questions in the future.

WTA is an important bacterial ligand for host receptors on mammalian immune cells with critical roles in innate immunity [8, 40]. WTA glycosylated with GlcNAc can activate the scavenger receptor langerin on skin Langerhans cells [41]. *S. aureus* is found on the skin of atopic dermatitis patients eliciting skin inflammation in a process that probably involves WTA-langerin interaction [8]. In contrast, *S. epidermidis* cannot activate langerin [41], probably because its GroP-WTA is glycosylated with glucose. It may be advantageous for *S. epidermidis*, one of the most abundant skin-colonizers [1], and for other CoNS, to avoid skin inflammation by producing a non-inflammatory WTA type decorated with glucose.

S. epidermidis uses the same pathway for GroP-WTA glycosylation with glucose residues as described for *B. subtilis* [28]. Activation of glucose via the PgcA and GtaB enzymes yields UDP-glucose as donor of glucose residues, which are subsequently transferred to the WTA backbone by TagE. Other WTA glycosyltransferases apart for TarM [27], including those transferring glucose to RboP-WTA in *B. subtilis* W23 (TarQ) [7, 11], GlcNAc to RboP-WTA in certain *S. aureus* clones (TarS, TarP) [11, 42], or GalNAc to GroP-WTA in *S. aureus* ST395 (TagN) [24] share no or very low similarity with TagE. However, protein structure prediction with Alphafold 2 revealed that TagE most likely forms a symmetric, propeller-like homotrimer with each monomer divided into the characteristic glycosyltransferase domain and the β-sheets containing trimerization domain as previously described for the well-studied *S. aureus* glycosyltransferase TarM (Fig. S5) [43-45].

In addition to glucose, WTA is usually also modified with D-alanine [38]. Since GroP repeating units have only one free hydroxyl group for substitution with either D-alanine or glucose, it is not surprising that only ca. 50% of the repeating units carried glucose residues. The teichoic acid D-alanylation machinery attaches D-alanine to a variety of different molecules including LTA, RboP-WTA, and GroP-WTA [46]. Its limited specificity for acceptor substrates may explain why a minor portion of the glucose residues on *S. epidermidis* GroP-WTA are also alanylated. GroP repeating units are shorter than RboP

repeating units, which may explain why the additional RboP-WTA polymers of *S. epidermidis* E73 are probably longer and precluded binding of ΦE72 to strain E73. The additional WTA may, therefore, represent a further strategy to interfere with phage infection and with interaction of other WTA-binding molecules.

Several other CoNS species appear to produce a similar WTA type as *S. epidermidis* because they encode potential TagE proteins and interact with ΦE72. Interspecies horizontal gene transfer via WTA-binding transducing phages appears to be rather common among these species and may have contributed to the import of the methicillin-resistance conferring *mecA* gene into *S. epidermidis* and, eventually, to *S. aureus* to create MRSE and MRSA clones [20]. It remains mysterious how the barrier for horizontal gene transfer between *S. epidermidis* and *S. aureus* that results from the substantial differences in WTA structure could be overcome. Specific *S. epidermidis* clonal lineages with both, GroP-WTA and *S. aureus*-type RboP-WTA such as ST10, ST23, and ST87 [6] or the *S. aureus* lineage ST395 producing CoNS-type GroP-WTA [14], may represent critical hubs for the exchange of genetic material between the species *S. epidermidis* and *S. aureus*. Several CoNS species encode potential WTA glycosyltransferase homologs with only low or no similarity to TagE. They may produce other WTA backbones or glycosylate their WTA with other sugars.

S. epidermidis often causes difficult-to-treat biofilm-based infections on implanted materials, which frequently require surgical replacement [4]. Treatment with lytic bacteriophages that could destroy *S. epidermidis* biofilms hold promise for the development of new therapeutic strategies [3, 18]. Understanding how phages detect suitable host bacteria and which *S. epidermidis* clones express corresponding phage-binding WTA motives will be important for the success of such strategies. The TagE-mediated WTA glycosylation with glucose might contribute to the narrow host range of lytic podoviruses like ΦBE03 [37]. Accordingly, finding podoviruses, which bind to GroP-WTA glucose might help to develop efficient therapeutic phage cocktails. Moreover, glycosylated WTA is a major antigen for protective antibodies against *S. aureus* [42, 47, 48] and, probably, also *S. epidermidis*. It represents therefore a particularly attractive antigen for vaccine development [48]. As for phage therapy, the success of such vaccination strategies will depend on in-depth knowledge on the structure and prevalence of WTA glycoepitopes among different *S. epidermidis* lineages. Our study may motivate more extensive investigations on WTA glycoepitopes in different staphylococcal pathogens and commensals.

Materials and Methods

Bacterial strains and growth conditions

S. epidermidis and *S. aureus* strains were cultivated in basic medium (BM) and incubated at 37°C on an orbital shaker. *E. coli* strains were cultivated in lysogeny broth (LB). Media were supplemented with appropriate antibiotics chloramphenicol (10 µg/ml), or ampicillin (100 µg/ml). *E. coli* DC10b and *S. aureus* PS187 Δ*sauUSI*Δ*hsdR* were used as cloning hosts, *S. epidermidis* 1457 was used for gene deletion studies. Bacteriophages and propagation strains used in this study are listed in Table S1.

Transposon mutagenesis of *S. epidermidis* strain 1457

The transposon plasmid pBTn described previously [25] was used to create a transposon library in *S. epidermidis* 1457. The features of this temperature-sensitive *E. coli/S. aureus* shuttle vector include a mini-transposon with an erythromycin resistance cassette flanked by inverted repeats from the horn fly transposon and a xylose-inducible transposase Himar1, which can mobilize the mini-transposon and integrate it into the chromosome with no bias for any specific sequence. Transposon library construction has been described in detail before [27]. In short, *S. epidermidis* 1457 was transformed with pBTn followed by mobilization of the mini-transposon into the genome upon xylose induction of the transposase. The pBTn plasmid was cured via shifts to nonpermissive temperature.

Isolation of phage-resistant transposon mutants

To isolate phage-resistant mutants, the transposon mutant library was infected with ΦE72 at a MOI of at least 100. After incubation for up to 4 h, the cells were centrifuged at 5,000 × g for 10 min and plated on TSA agar containing erythromycin. Single colonies of surviving mutants were transferred to fresh TSA agar plates repeatedly. Phage resistance was confirmed by spot assays with ΦE72, and the phage-resistant mutants were treated with 1 µg/ml mitomycin to test for and to exclude lysogeny. To identify the site of transposon insertion, total DNA was isolated, purified with the NucleoSpin® tissue kit (Macherey-Nagel, Düren), digested, religated, multiplied with primers erm-For and erm-Rev (Table S2), which anneal to the erythromycin resistance cassette of the mini-transposon, and sequenced.

Molecular genetic methods

For the construction of the *tagE*, *pgcA,* and *gtaB* mutants in *S. epidermidis* 1457, the pBASE6 *E. coli/S.aureus* shuttle vector was used according to standard procedures [49]. For mutant complementation, plasmid pRB473 was used [50]. The primers for knockout and complementation plasmid construction are listed in (Table S2). Both pBASE6 and pRB473 containing either the respective up- and downstream fragments for knockout construction (pBASE6) or the complementation sequence (pRB473), were used to transform *E. coli* DC10b, and subsequently PS187 Δ*sauUSI*Δ*hsdR* by electroporation. The plasmids were subsequently transferred to *S. epidermidis* strain 1457 by

transduction with Φ187 using *S. aureus* PS187 Δ*sauUSI*Δ*hsdR* as donor strain as described previously [51].

Phage binding, infection, and transduction assays

Phage spot assays were performed as described previously [14]. All applied bacteriophages (Table S1) were propagated in suitable bacterial host strains and phage lysates were filtered to yield sterile phage suspensions. Test bacteria were cultivated overnight in fresh BM. OD_{600} = 0.1 was adjusted in 5 ml LB soft agar for the preparation of bacterial overlay lawns. 10 µl of phage suspensions were spotted onto the bacterial lawns. After overnight incubation at 37°C for podoviruses and siphoviruses, and 30°C for myoviruses, phage clearing zones and individual plaques were observed and recorded.

Phage adsorption efficiency was determined as described previously with minor modifications [14]. Briefly, adsorption rates were analyzed by mixing approximately 10^6 PFU/ml in BM supplemented with 4 mM $CaCl_2$ with the tested bacteria at an OD_{600} of 0.5 and incubating for 15 min at 37°C. The samples were subsequently centrifuged, and the supernatants were spotted on indicator strains to determine the number of unbound phages in the supernatant. The adsorption rate was calculated by dividing the number of bound phages by the number of input phages.

Transduction experiments were performed as described previously [14]. Briefly, 1 ml of exponentially growing cultures of a recipient strain was adjusted to an OD_{600} of 0.5. The cells were sedimented by centrifugation and resuspended in 200 µl of phage buffer containing 0.1% gelatin, 1 mM $MgSO_4$, 4 mM $CaCl_2$, 50 mM Tris, and 0.1 M NaCl. 200 µl of bacteria in phage buffer were mixed with 100 µl of lysates obtained from *S. aureus* PS187 and *S. epidermidis* 1457 donor strains carrying plasmids of choice. Samples were then incubated for 15 min at 37°C, diluted, and plated on chloramphenicol-containing BM agar to count colonies.

Electron microscopy

S. epidermidis 1457 wild type, *ΔtagE*, *ΔpgcA*, and *ΔgtaB* were grown until stationary phase, and fixed at an OD_{600} of 10 in 200 µl Karnovsky's fixative (3% formaldehyde, 2.5% glutaraldehyde in 0.1 M phosphate buffer pH 7.4) for 24 h. Samples were then centrifuged at 1,400 x g for 5 min, supernatant was discarded, pellets were resuspended in approximately 20 µl agarose (3.9%) at 37°C, cooled to room temperature, and cut into small pieces. Postfixation was based on 1.0% osmium tetroxide containing 2.5% potassium ferrocyanide (Morphisto) for 2 h. After following the standard methods, samples were embedded in glycide ether and cut using an ultramicrotome (Ultracut E, Reichert). Ultra-thin sections (30 nm) were mounted on copper grids and analyzed using a Zeiss LIBRA 120 transmission electron microscope (Carl Zeiss) operating at 120 kV.

WTA isolation

WTA was isolated as described previously [14, 52, 53] with minor modifications. Briefly, bacterial cells from two liters of overnight cultures were washed and disrupted with glass beads in a cell disrupter (Euler). Cell lysates were incubated at 37°C overnight in the presence of DNase and RNase. SDS was added to a final concentration of 2% followed by ultrasonication for 15 min. Cell walls were washed several times to remove SDS. To release WTA from cell walls, samples were treated with 5% trichloroacetic acid for 4 h at 65°C. Peptidoglycan debris was separated via centrifugation (10 min, 14,500 x g). Determination of phosphate amounts as described previously [53-55] was used for WTA quantification. Crude WTA extracts were further purified as already described [27]. Briefly, the pH of the crude extract was adjusted to 5 with NaOH and dialyzed against water with a Slide-A-Lyzer Dialysis Cassette (MWCO of 3.5 kDa; Thermo Fisher Scientific). For HPLC-MS analysis, 50 µl of 100 mM WTA sample were hydrolyzed with 100 mM NaOH at 60°C for 2 h. The remaining dialyzed WTA was further lyophilized for long-term storage at -20 °C or used for further analysis. 10-15 mg lyophilized WTA sample were used for NMR. Detailed explanations of the HPLC-MS and NMR methods can be found as extended descriptions of detailed methods.

Enzymatic determination of glucose in the WTA samples

The High Sensitivity Glucose Assay Kit (mak181, Sigma-Aldrich) was used to determine the glucose content in the WTA sample. 50 µl of dialyzed WTA samples and 50 µl of 1 mM glucose standard solution were dried in a vacuum concentrator at 60°C. 100 µl of 0.5 M HCl was added to the samples and the standard solution and cooked for 2 h in a water bath. The glucose standard was diluted 1:50 resulting in a 10 µM concentration and different volumes were used to cover a range of 0 - 100 pmol. Samples were also diluted at least 1:50 and different dilutions of the samples were tested in a 96-well plate. The assay was performed according to the manufacturer's instructions. The fluorescence intensity was measured at excitation wavelength 535 nm and emission wavelength 587 nm.

Glycolipid isolation, thin layer chromatography (TLC) and detection with α-naphthol

The detection of glycolipids was performed similar to a previously described method [36]. *S. epidermidis* 1457 and the respective mutants were grown to OD_{600} of 3.5. 5 ml of bacterial suspension were washed and resuspended in 500 µl of 100 mM sodiumacetate (pH 4.7) and transferred into glass vials. 500 µl chloroform and 500 ml methanol were added and the mixture was vortexed vigorously. The samples were centrifuged at 4,600 x g for 20 min at 4°C and the lower phase was dried overnight and resuspended in 25 µl methanol and chloroform in a 1:1 ratio. The whole sample was applied to a high-performance thin-layer chromatography (HPTLC) silica gel 60 plate (10 x 10 cm; Merck) with a Hamilton syringe. A positive control containing 5 µg digalactosyldiacylglycerol (DGDG, Sigma-Aldrich)

was used. A Linomat 5 (Camag), and an auto developing chamber (Camag), were used to apply the sample to the TLC plate and to run it with a solvent containing 65:25:4 (v/v/v) chloroform/methanol/H_2O. The dried TLC plate was sprayed with 3.2% α-naphthol in methanol/H_2SO_4/H_2O 25:3:2 (v/v/v) and the glycolipids were visualized by heating the plate at 110°C for a few minutes.

In silico **analysis**

All statistical analyses were performed with Graph Pad Prism 9.2.0 (GraphPad Software, La Jolla, USA). Multiple sequence alignment was performed with SnapGene® 5.3.2 using MUSCLE. Protein structure prediction was done using AlphaFold2 with ColabFold [44, 45].

Acknowledgements

We thank David Gerlach, Xin Du, and Bernhard Krismer for helpful discussions, Arnaud Kengmo Tchoupa and Ulrike Redel for help with TLC, and Y. Que and E. Baumgartner for supply of phages. This work was financed by grants from the German Research Foundation to A.P. (TRR34; TRR165 project ID 246807620; PE 805/7-1 project ID 410190180; PE 805/8-1 project ID 410190180) and the German Center for Infection Research (DZIF) to A.P. The authors acknowledge infrastructural support by the Cluster of Excellence EXC 2124 ‘Controlling Microbes to Fight Infections’ project ID 39083813

References

1. Severn MM, Horswill AR. Staphylococcus epidermidis and its dual lifestyle in skin health and infection. Nat Rev Microbiol. 2022. Epub 20220830. doi: 10.1038/s41579-022-00780-3. PubMed PMID: 36042296.
2. Otto M. Staphylococcus epidermidis--the 'accidental' pathogen. Nat Rev Microbiol. 2009;7(8):555-67. doi: 10.1038/nrmicro2182. PubMed PMID: 19609257; PubMed Central PMCID: PMCPMC2807625.
3. Schilcher K, Horswill AR. Staphylococcal Biofilm Development: Structure, Regulation, and Treatment Strategies. Microbiol Mol Biol Rev. 2020;84(3). Epub 20200812. doi: 10.1128/mmbr.00026-19. PubMed PMID: 32792334; PubMed Central PMCID: PMCPMC7430342.
4. Becker K, Heilmann C, Peters G. Coagulase-negative staphylococci. Clin Microbiol Rev. 2014;27(4):870-926. doi: 10.1128/CMR.00109-13. PubMed PMID: 25278577; PubMed Central PMCID: PMCPMC4187637.
5. Otto M. Staphylococcal Biofilms. Microbiol Spectr. 2018;6(4). doi: 10.1128/microbiolspec.GPP3-0023-2018. PubMed PMID: 30117414; PubMed Central PMCID: PMCPMC6282163.
6. Du X, Larsen J, Li M, Walter A, Slavetinsky C, Both A, et al. Staphylococcus epidermidis clones express Staphylococcus aureus-type wall teichoic acid to shift from a commensal to pathogen lifestyle. Nat Microbiol. 2021;6(6):757-68. Epub 20210524. doi: 10.1038/s41564-021-00913-z. PubMed PMID: 34031577.
7. Brown S, Santa Maria JP, Jr., Walker S. Wall teichoic acids of gram-positive bacteria. Annu Rev Microbiol. 2013;67:313-36. doi: 10.1146/annurev-micro-092412-155620. PubMed PMID: 24024634; PubMed Central PMCID: PMCPMC3883102.
8. van Dalen R, Peschel A, van Sorge NM. Wall Teichoic Acid in Staphylococcus aureus Host Interaction. Trends Microbiol. 2020;28(12):985-98. Epub 20200612. doi: 10.1016/j.tim.2020.05.017. PubMed PMID: 32540314.
9. Endl J, Seidl HP, Fiedler F, Schleifer KH. Chemical composition and structure of cell wall teichoic acids of staphylococci. Arch Microbiol. 1983;135(3):215-23. doi: 10.1007/BF00414483. PubMed PMID: 6639273.
10. Ingmer H, Gerlach D, Wolz C. Temperate Phages of Staphylococcus aureus. Microbiol Spectr. 2019;7(5). Epub 2019/09/29. doi: 10.1128/microbiolspec.GPP3-0058-2018. PubMed PMID: 31562736.
11. Brown S, Xia G, Luhachack LG, Campbell J, Meredith TC, Chen C, et al. Methicillin resistance in Staphylococcus aureus requires glycosylated wall teichoic acids. Proc Natl Acad Sci U S A. 2012;109(46):18909-14. Epub 20121001. doi: 10.1073/pnas.1209126109. PubMed PMID: 23027967; PubMed Central PMCID: PMCPMC3503181.
12. Gerlach D, Sieber RN, Larsen J, Krusche J, De Castro C, Baumann J, et al. Horizontal transfer and phylogenetic distribution of the immune evasion factor tarP. Front Microbiol. 2022;13:951333. Epub 20221028. doi: 10.3389/fmicb.2022.951333. PubMed PMID: 36386695; PubMed Central PMCID: PMCPMC9650247.
13. Li X, Gerlach D, Du X, Larsen J, Stegger M, Kühner P, et al. An accessory wall teichoic acid glycosyltransferase protects Staphylococcus aureus from the lytic activity of Podoviridae. Sci Rep. 2015;5:17219. Epub 20151124. doi: 10.1038/srep17219. PubMed PMID: 26596631; PubMed Central PMCID: PMCPMC4667565.
14. Winstel V, Liang C, Sanchez-Carballo P, Steglich M, Munar M, Bröker BM, et al. Wall teichoic acid structure governs horizontal gene transfer between major bacterial pathogens. Nat Commun. 2013;4:2345. doi: 10.1038/ncomms3345. PubMed PMID: 23965785; PubMed Central PMCID: PMCPMC3903184.
15. Xia G, Corrigan RM, Winstel V, Goerke C, Gründling A, Peschel A. Wall teichoic Acid-dependent adsorption of staphylococcal siphovirus and myovirus. J Bacteriol. 2011;193(15):4006-9.

423 Epub 20110603. doi: 10.1128/jb.01412-10. PubMed PMID: 21642458; PubMed Central PMCID:
424 PMCPMC3147540.
425 16. O'Flaherty S, Ross RP, Meaney W, Fitzgerald GF, Elbreki MF, Coffey A. Potential of the
426 polyvalent anti-Staphylococcus bacteriophage K for control of antibiotic-resistant staphylococci from
427 hospitals. Appl Environ Microbiol. 2005;71(4):1836-42. doi: 10.1128/aem.71.4.1836-1842.2005.
428 PubMed PMID: 15812009; PubMed Central PMCID: PMCPMC1082512.
429 17. Cerca N, Oliveira R, Azeredo J. Susceptibility of Staphylococcus epidermidis planktonic cells
430 and biofilms to the lytic action of staphylococcus bacteriophage K. Lett Appl Microbiol.
431 2007;45(3):313-7. doi: 10.1111/j.1472-765X.2007.02190.x. PubMed PMID: 17718845.
432 18. Kilcher S, Loessner MJ. Engineering Bacteriophages as Versatile Biologics. Trends Microbiol.
433 2019;27(4):355-67. Epub 20181012. doi: 10.1016/j.tim.2018.09.006. PubMed PMID: 30322741.
434 19. Winstel V, Kühner P, Rohde H, Peschel A. Genetic engineering of untransformable coagulase-
435 negative staphylococcal pathogens. Nat Protoc. 2016;11(5):949-59. Epub 20160421. doi:
436 10.1038/nprot.2016.058. PubMed PMID: 27101516.
437 20. Rolo J, Worning P, Nielsen JB, Bowden R, Bouchami O, Damborg P, et al. Evolutionary Origin
438 of the Staphylococcal Cassette Chromosome mec (SCCmec). Antimicrob Agents Chemother.
439 2017;61(6). Epub 20170524. doi: 10.1128/AAC.02302-16. PubMed PMID: 28373201; PubMed Central
440 PMCID: PMCPMC5444190.
441 21. Lee AS, de Lencastre H, Garau J, Kluytmans J, Malhotra-Kumar S, Peschel A, et al. Methicillin-
442 resistant Staphylococcus aureus. Nat Rev Dis Primers. 2018;4:18033. Epub 2018/06/01. doi:
443 10.1038/nrdp.2018.33. PubMed PMID: 29849094.
444 22. Fisarova L, Botka T, Du X, Maslanova I, Bardy P, Pantucek R, et al. Staphylococcus epidermidis
445 Phages Transduce Antimicrobial Resistance Plasmids and Mobilize Chromosomal Islands. mSphere.
446 2021;6(3). Epub 2021/05/14. doi: 10.1128/mSphere.00223-21. PubMed PMID: 33980677.
447 23. Fanaei Pirlar R, Wagemans J, Ponce Benavente L, Lavigne R, Trampuz A, Gonzalez Moreno M.
448 Novel Bacteriophage Specific against Staphylococcus epidermidis and with Antibiofilm Activity.
449 Viruses. 2022;14(6). Epub 20220620. doi: 10.3390/v14061340. PubMed PMID: 35746811; PubMed
450 Central PMCID: PMCPMC9230115.
451 24. Winstel V, Sanchez-Carballo P, Holst O, Xia G, Peschel A. Biosynthesis of the unique wall
452 teichoic acid of Staphylococcus aureus lineage ST395. mBio. 2014;5(2):e00869. Epub 20140408. doi:
453 10.1128/mBio.00869-14. PubMed PMID: 24713320; PubMed Central PMCID: PMCPMC3993852.
454 25. Li M, Rigby K, Lai Y, Nair V, Peschel A, Schittek B, et al. Staphylococcus aureus mutant screen
455 reveals interaction of the human antimicrobial peptide dermcidin with membrane phospholipids.
456 Antimicrob Agents Chemother. 2009;53(10):4200-10. Epub 20090713. doi: 10.1128/aac.00428-09.
457 PubMed PMID: 19596877; PubMed Central PMCID: PMCPMC2764178.
458 26. Allison SE, D'Elia MA, Arar S, Monteiro MA, Brown ED. Studies of the genetics, function, and
459 kinetic mechanism of TagE, the wall teichoic acid glycosyltransferase in Bacillus subtilis 168. J Biol
460 Chem. 2011;286(27):23708-16. Epub 20110510. doi: 10.1074/jbc.M111.241265. PubMed PMID:
461 21558268; PubMed Central PMCID: PMCPMC3129151.
462 27. Xia G, Maier L, Sanchez-Carballo P, Li M, Otto M, Holst O, et al. Glycosylation of wall teichoic
463 acid in Staphylococcus aureus by TarM. J Biol Chem. 2010;285(18):13405-15. Epub 20100225. doi:
464 10.1074/jbc.M109.096172. PubMed PMID: 20185825; PubMed Central PMCID: PMCPMC2859500.
465 28. Lazarevic V, Soldo B, Médico N, Pooley H, Bron S, Karamata D. Bacillus subtilis alpha-
466 phosphoglucomutase is required for normal cell morphology and biofilm formation. Appl Environ
467 Microbiol. 2005;71(1):39-45. doi: 10.1128/aem.71.1.39-45.2005. PubMed PMID: 15640167; PubMed
468 Central PMCID: PMCPMC544238.
469 29. Pooley HM, Paschoud D, Karamata D. The gtaB marker in Bacillus subtilis 168 is associated
470 with a deficiency in UDPglucose pyrophosphorylase. J Gen Microbiol. 1987;133(12):3481-93. doi:
471 10.1099/00221287-133-12-3481. PubMed PMID: 2846750.
472 30. Yasbin RE, Maino VC, Young FE. Bacteriophage resistance in Bacillus subtilis 168, W23, and
473 interstrain transformants. J Bacteriol. 1976;125(3):1120-6. doi: 10.1128/jb.125.3.1120-1126.1976.
474 PubMed PMID: 815237; PubMed Central PMCID: PMCPMC236191.

31. Qian Z, Yin Y, Zhang Y, Lu L, Li Y, Jiang Y. Genomic characterization of ribitol teichoic acid synthesis in Staphylococcus aureus: genes, genomic organization and gene duplication. BMC Genomics. 2006;7(1):74. doi: 10.1186/1471-2164-7-74.
32. Swoboda JG, Campbell J, Meredith TC, Walker S. Wall teichoic acid function, biosynthesis, and inhibition. Chembiochem. 2010;11(1):35-45. doi: 10.1002/cbic.200900557. PubMed PMID: 19899094; PubMed Central PMCID: PMCPMC2798926.
33. Jorasch P, Wolter FP, Zähringer U, Heinz E. A UDP glucosyltransferase from Bacillus subtilis successively transfers up to four glucose residues to 1,2-diacylglycerol: expression of ypfP in Escherichia coli and structural analysis of its reaction products. Mol Microbiol. 1998;29(2):419-30. doi: 10.1046/j.1365-2958.1998.00930.x. PubMed PMID: 9720862.
34. Kiriukhin MY, Debabov DV, Shinabarger DL, Neuhaus FC. Biosynthesis of the glycolipid anchor in lipoteichoic acid of Staphylococcus aureus RN4220: role of YpfP, the diglucosyldiacylglycerol synthase. J Bacteriol. 2001;183(11):3506-14. doi: 10.1128/jb.183.11.3506-3514.2001. PubMed PMID: 11344159; PubMed Central PMCID: PMCPMC99649.
35. Fedtke I, Mader D, Kohler T, Moll H, Nicholson G, Biswas R, et al. A Staphylococcus aureus ypfP mutant with strongly reduced lipoteichoic acid (LTA) content: LTA governs bacterial surface properties and autolysin activity. Mol Microbiol. 2007;65(4):1078-91. Epub 20070719. doi: 10.1111/j.1365-2958.2007.05854.x. PubMed PMID: 17640274; PubMed Central PMCID: PMCPMC2169524.
36. Gründling A, Schneewind O. Genes required for glycolipid synthesis and lipoteichoic acid anchoring in Staphylococcus aureus. J Bacteriol. 2007;189(6):2521-30. Epub 20070105. doi: 10.1128/jb.01683-06. PubMed PMID: 17209021; PubMed Central PMCID: PMCPMC1899383.
37. Valente LG, Pitton M, Fürholz M, Oberhaensli S, Bruggmann R, Leib SL, et al. Isolation and characterization of bacteriophages from the human skin microbiome that infect Staphylococcus epidermidis. FEMS Microbes. 2021;2. doi: 10.1093/femsmc/xtab003.
38. Weidenmaier C, Peschel A. Teichoic acids and related cell-wall glycopolymers in Gram-positive physiology and host interactions. Nat Rev Microbiol. 2008;6(4):276-87. Epub 2008/03/11. doi: 10.1038/nrmicro1861. PubMed PMID: 18327271.
39. Goller PC, Elsener T, Lorge D, Radulovic N, Bernardi V, Naumann A, et al. Multi-species host range of staphylococcal phages isolated from wastewater. Nat Commun. 2021;12(1):6965. Epub 20211129. doi: 10.1038/s41467-021-27037-6. PubMed PMID: 34845206; PubMed Central PMCID: PMCPMC8629997.
40. Schade J, Weidenmaier C. Cell wall glycopolymers of Firmicutes and their role as nonprotein adhesins. FEBS Lett. 2016;590(21):3758-71. Epub 20160725. doi: 10.1002/1873-3468.12288. PubMed PMID: 27396949.
41. van Dalen R, De La Cruz Diaz JS, Rumpret M, Fuchsberger FF, van Teijlingen NH, Hanske J, et al. Langerhans Cells Sense Staphylococcus aureus Wall Teichoic Acid through Langerin To Induce Inflammatory Responses. mBio. 2019;10(3). Epub 20190514. doi: 10.1128/mBio.00330-19. PubMed PMID: 31088921; PubMed Central PMCID: PMCPMC6520447.
42. Gerlach D, Guo Y, De Castro C, Kim SH, Schlatterer K, Xu FF, et al. Methicillin-resistant Staphylococcus aureus alters cell wall glycosylation to evade immunity. Nature. 2018;563(7733):705-9. Epub 20181121. doi: 10.1038/s41586-018-0730-x. PubMed PMID: 30464342.
43. Koc C, Gerlach D, Beck S, Peschel A, Xia G, Stehle T. Structural and enzymatic analysis of TarM glycosyltransferase from Staphylococcus aureus reveals an oligomeric protein specific for the glycosylation of wall teichoic acid. J Biol Chem. 2015;290(15):9874-85. Epub 20150219. doi: 10.1074/jbc.M114.619924. PubMed PMID: 25697358; PubMed Central PMCID: PMCPMC4392284.
44. Jumper J, Evans R, Pritzel A, Green T, Figurnov M, Ronneberger O, et al. Highly accurate protein structure prediction with AlphaFold. Nature. 2021;596(7873):583-9. Epub 20210715. doi: 10.1038/s41586-021-03819-2. PubMed PMID: 34265844; PubMed Central PMCID: PMCPMC8371605.

525 45. Mirdita M, Schütze K, Moriwaki Y, Heo L, Ovchinnikov S, Steinegger M. ColabFold: making
526 protein folding accessible to all. Nature Methods. 2022;19(6):679-82. doi: 10.1038/s41592-022-
527 01488-1.
528 46. Schultz BJ, Snow ED, Walker S. Mechanism of D-alanine transfer to teichoic acids shows how
529 bacteria acylate cell envelope polymers. Nat Microbiol. 2023. Epub 20230612. doi: 10.1038/s41564-
530 023-01411-0. PubMed PMID: 37308592.
531 47. Kurokawa K, Jung DJ, An JH, Fuchs K, Jeon YJ, Kim NH, et al. Glycoepitopes of staphylococcal
532 wall teichoic acid govern complement-mediated opsonophagocytosis via human serum antibody and
533 mannose-binding lectin. J Biol Chem. 2013;288(43):30956-68. Epub 20130917. doi:
534 10.1074/jbc.M113.509893. PubMed PMID: 24045948; PubMed Central PMCID: PMCPMC3829409.
535 48. van Dalen R, Molendijk MM, Ali S, van Kessel KPM, Aerts P, van Strijp JAG, et al. Do not
536 discard Staphylococcus aureus WTA as a vaccine antigen. Nature. 2019;572(7767):E1-e2. Epub
537 20190731. doi: 10.1038/s41586-019-1416-8. PubMed PMID: 31367020.
538 49. Geiger T, Francois P, Liebeke M, Fraunholz M, Goerke C, Krismer B, et al. The stringent
539 response of Staphylococcus aureus and its impact on survival after phagocytosis through the
540 induction of intracellular PSMs expression. PLoS Pathog. 2012;8(11):e1003016. Epub 20121129. doi:
541 10.1371/journal.ppat.1003016. PubMed PMID: 23209405; PubMed Central PMCID:
542 PMCPMC3510239.
543 50. Brückner R. A series of shuttle vectors for Bacillus subtilis and Escherichia coli. Gene.
544 1992;122(1):187-92. doi: 10.1016/0378-1119(92)90048-t. PubMed PMID: 1452028.
545 51. Winstel V, Kühner P, Rohde H, Peschel A. Genetic engineering of untransformable coagulase-
546 negative staphylococcal pathogens. Nature Protocols. 2016;11(5):949-59. doi:
547 10.1038/nprot.2016.058.
548 52. Weidenmaier C, Kokai-Kun JF, Kristian SA, Chanturiya T, Kalbacher H, Gross M, et al. Role of
549 teichoic acids in Staphylococcus aureus nasal colonization, a major risk factor in nosocomial
550 infections. Nat Med. 2004;10(3):243-5. Epub 20040201. doi: 10.1038/nm991. PubMed PMID:
551 14758355.
552 53. Peschel A, Otto M, Jack RW, Kalbacher H, Jung G, Gotz F. Inactivation of the dlt operon in
553 Staphylococcus aureus confers sensitivity to defensins, protegrins, and other antimicrobial peptides.
554 J Biol Chem. 1999;274(13):8405-10. doi: 10.1074/jbc.274.13.8405. PubMed PMID: 10085071.
555 54. Chen PS, Toribara TY, Warner H. Microdetermination of Phosphorus. Analytical Chemistry.
556 1956;28:1756-8.
557 55. Chen PS, Toribara TY, Warner H. Microdetermination of Phosphorus. Analytical Chemistry.
558 1956;28(11):1756-8. doi: 10.1021/ac60119a033.
559 56. Kontou EE, Walter A, Alka O, Pfeuffer J, Sachsenberg T, Mohite OS, et al. UmetaFlow: an
560 untargeted metabolomics workflow for high-throughput data processing and analysis. Journal of
561 Cheminformatics. 2023;15(1):52. doi: 10.1186/s13321-023-00724-w.
562 57. Speciale I, Notaro A, Garcia-Vello P, Di Lorenzo F, Armiento S, Molinaro A, et al. Liquid-state
563 NMR spectroscopy for complex carbohydrate structural analysis: A hitchhiker's guide. Carbohydrate
564 Polymers. 2022;277:118885. doi: https://doi.org/10.1016/j.carbpol.2021.118885.
565 58. Garcia-Vello P, Sharma G, Speciale I, Molinaro A, Im SH, De Castro C. Structural features and
566 immunological perception of the cell surface glycans of Lactobacillus plantarum: a novel rhamnose-
567 rich polysaccharide and teichoic acids. Carbohydr Polym. 2020;233:115857. Epub 20200110. doi:
568 10.1016/j.carbpol.2020.115857. PubMed PMID: 32059908.

569

570

Figures

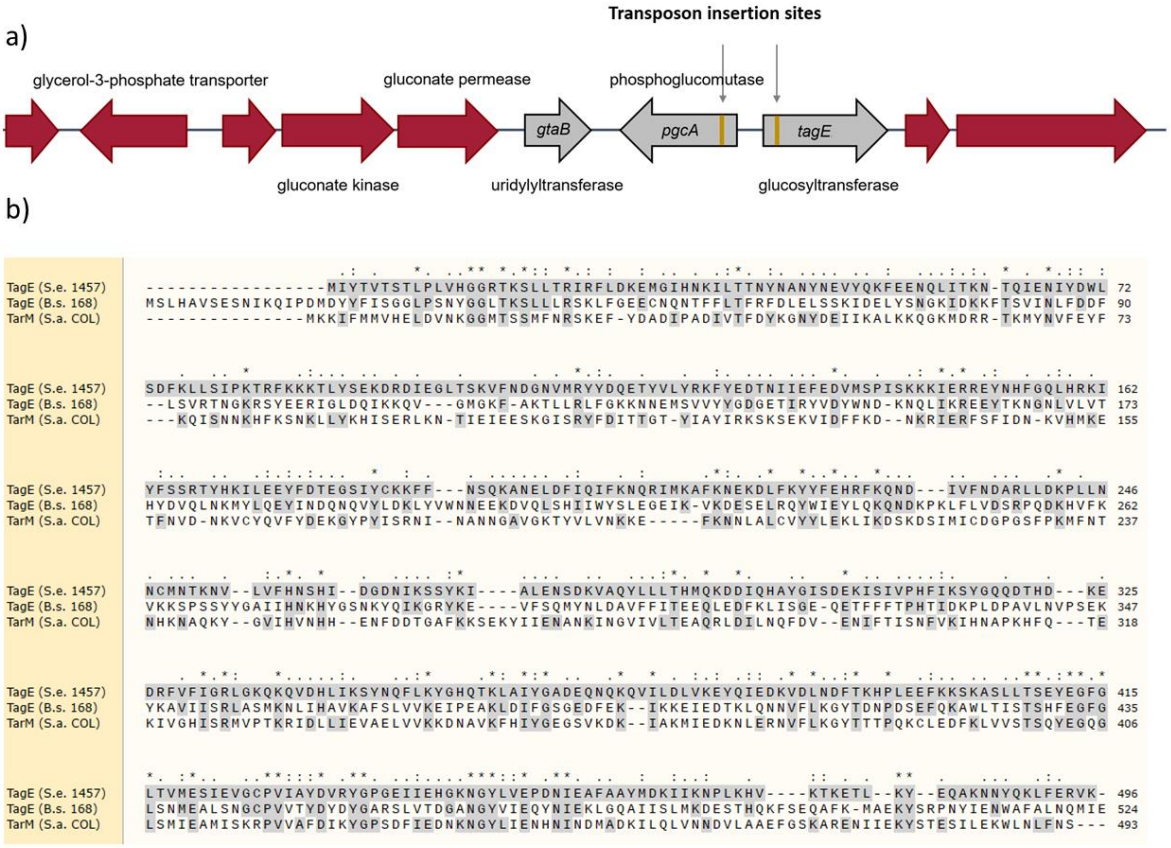

Figure 1: The *tagE* gene encodes a glycosyltransferase in *S. epidermidis*. a) Genetic locus identified by transposon mutagenesis contains the *S. epidermidis tagE, pgcA,* and *gtaB* homologues. Transposon insertion sites are labeled in gold. b) MUSCLE alignment of *S. epidermidis* TagE with *B. subtilis* TagE and *S. aureus* TarM protein sequences.

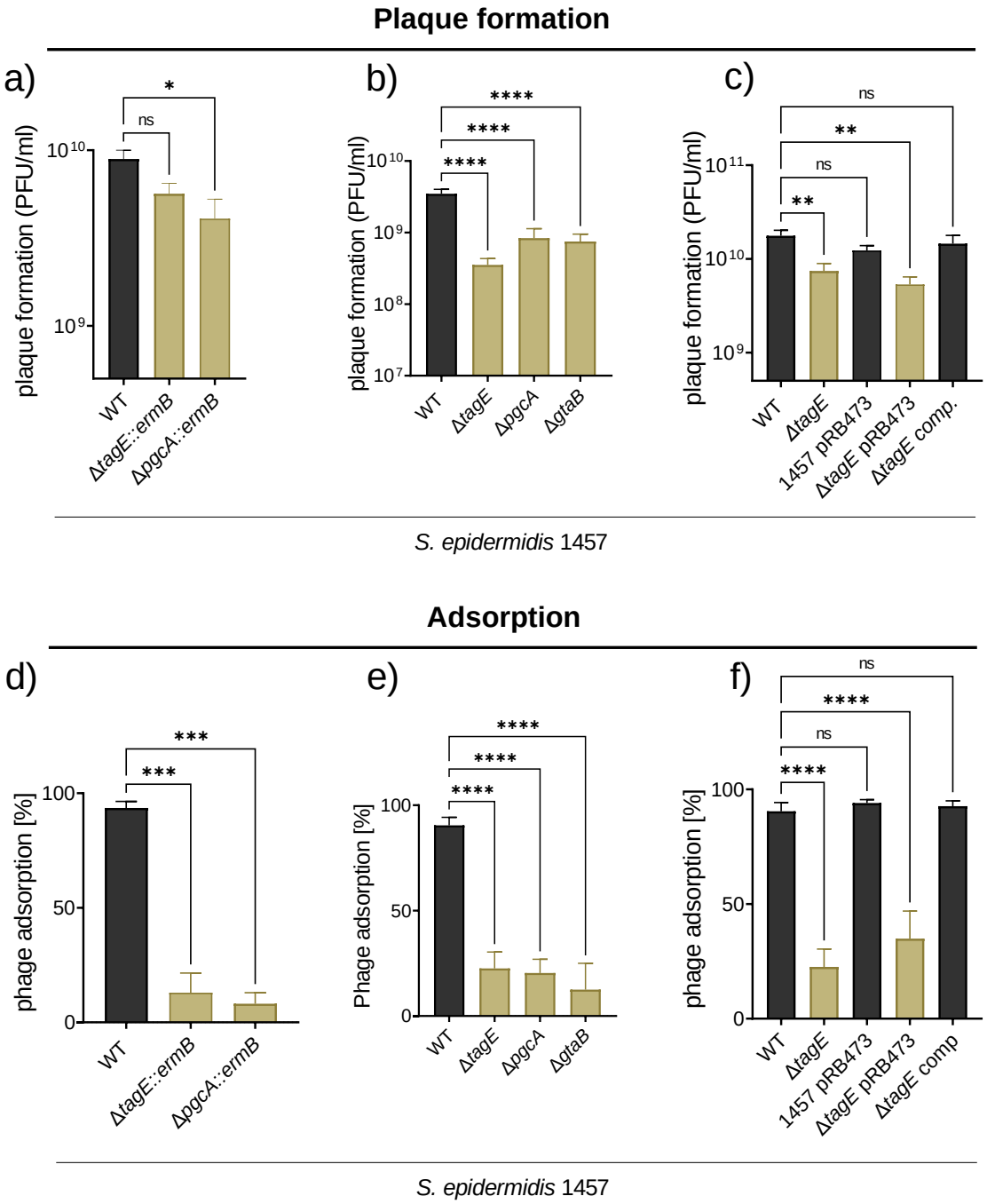

Figure 2: ΦE72 shows decreased infection (a,b) and binding (d,e) of the *tagE*, *pgcA,* and *gtaB* mutants. This deffect can be restored by complementing the *tagE* mutant with the genetic locus containing *tagE*, *pgcA,* and *gtaB* on plasmid pRB473 (c,f). The data represent the mean ± SEM of at least three independent experiments. Ordinary one-way ANOVA was used to determine statistical significance versus *S. epidermidis* 1457 wild type (WT), indicated as: not significant (ns), $^{*}P < 0.05$, $^{**}P < 0.01$, $^{***}P < 0.001$, $^{****}P < 0.0001$.

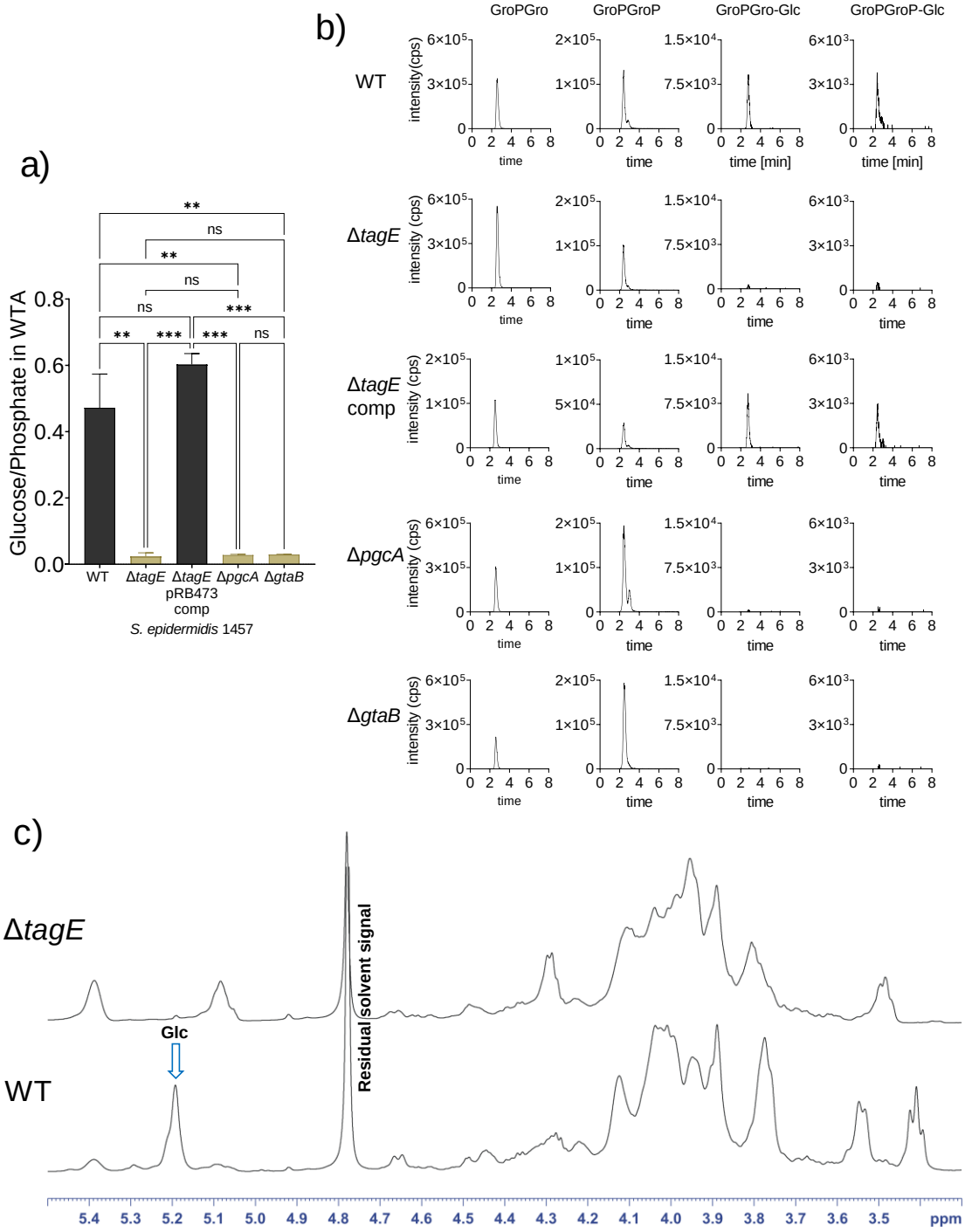

584

585 **Figure 3:** WTA analysis of the *S. epidermidis* mutants Δ*tagE*, Δ*pgcA,* Δ*gtaB* and of Δ*tagE* containing the
586 pRB473 plasmid carrying *tagE, pgcA, and gtaB* genes for complementation. a) Ratio of glucose per
587 phosphate content of WTA measured enzymatically. b) HPLC-MS: Extracted ion chromatograms (EIC)
588 of GroP-Gro ($[M - H]^-$ = 245.0432) and GroP-GroP ($[M - H]^-$ = 325.0095) with (GroP-Gro-Glc; $[M - H]^-$ =
589 407.096) (GroP-GroP-Glc; $[M - H]^-$ = 487.0623) or without glucose substitution. c) ^{1}H NMR spectra
590 reveal D-glucose on WTA of the *S. epidermidis* 1457 wild type (WT) (at the C2-position of GroP), while
591 deletion of *tagE* results in absence of glucose on WTA. For a) data represent the mean ± SEM of at
592 least three independent experiments. Ordinary one-way ANOVA was used to determine statistical
593 significance, indicated as: not significant (ns), $^{**}P < 0.01$, $^{***}P < 0.001$.

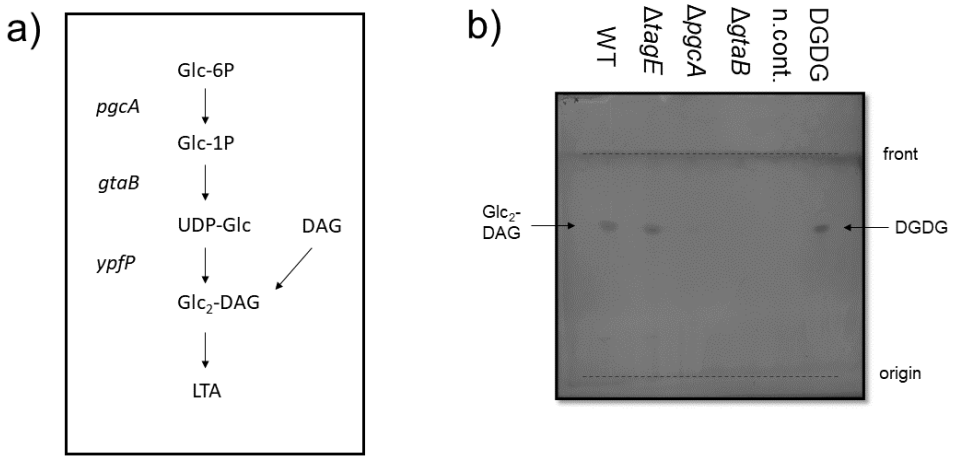

Figure 4: Glycolipid detection by TLC. a) LTA glycolipid biosynthesis pathway as described for *S. aureus* and *B. subtilis* (adapted from [36]). b) Glycolipid detection on a TLC plate stained with α-naphtol/sulfuric acid. 5 µg of digalactosyldiacylglycerol (DGDG) was used as positive control, the solvent methanol/chloroform (1:1) as negative control (n.cont.). One representative experiment of three independent experiments is shown.

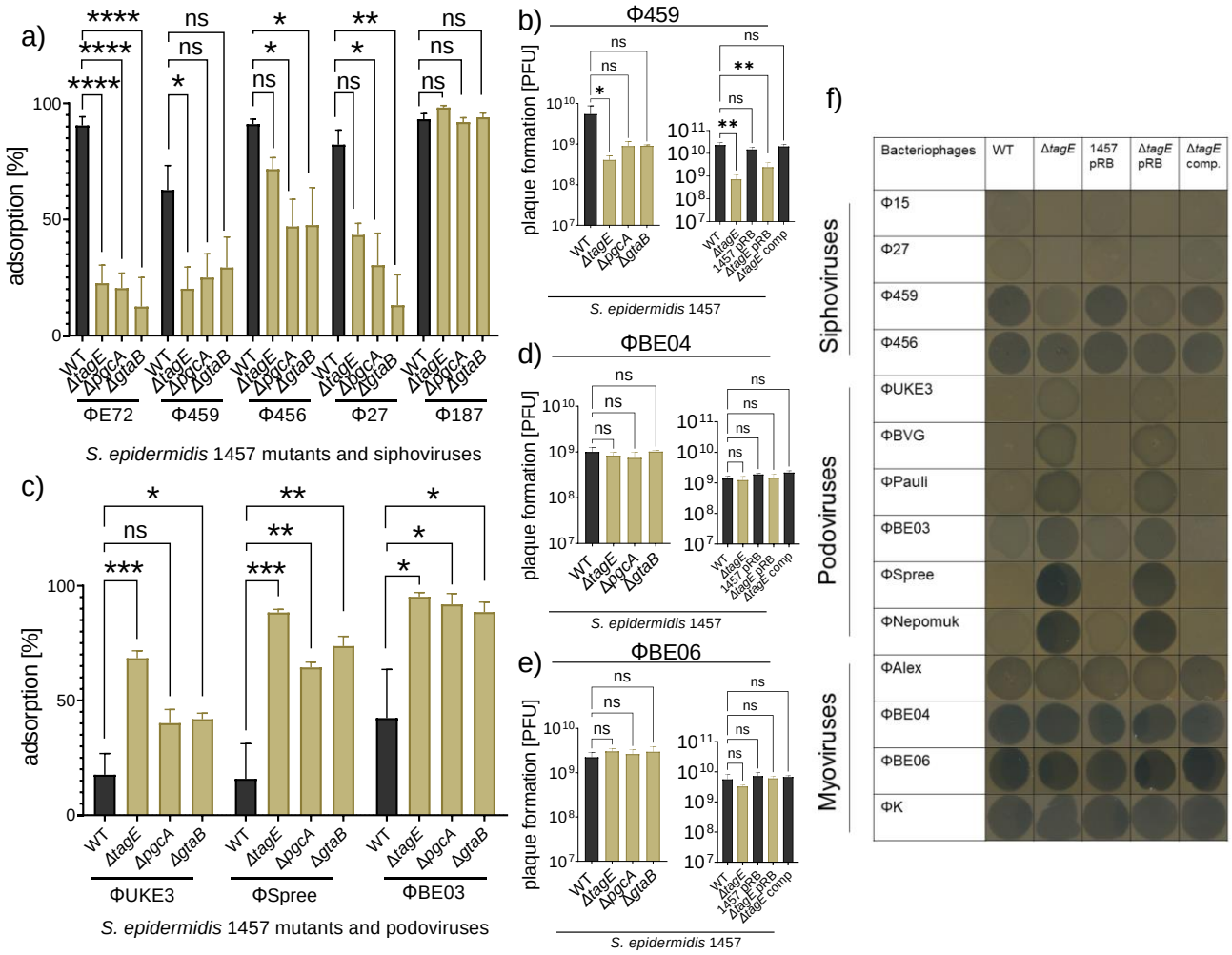

Figure 5: TagE-glycosylated WTA increases binding of siphoviruses but reduces podovirus binding. WTA glycosylation-deficient mutants of *S. epidermidis* show decreased binding of ΦE72-related siphoviruses Φ459, Φ456, and Φ27 (a), but increased binding of the podoviruses ΦUKE3, ΦSpree, and ΦBE03 (c), while the GroP-GalNAc-specific siphovirus Φ187 still shows strong binding (a). WTA glycosylation-deficient mutants of *S. epidermidis* show less plaque formation by ΦE72-related siphovirus Φ459 (b), while plaque formation by the myoviruses ΦBE04 (d) and ΦBE06 (e) remains unchanged. f) Lytic zones and "lysis from without" by siphoviruses decrease in the absence of *tagE* but increase for podoviruses. Myoviruses show formation of lytic zones independently of the presence or absence of *tagE*. (pRB= pRB473 (empty vector control); comp = complementation with *tagE*, *gtaB*, *pgcA* genes) The data represents the mean ± SEM of at least three independent experiments. Ordinary one-way ANOVA was used to determine statistical significance versus *S. epidermidis* 1457 wild type (WT), indicated as: not significant (ns), *P < 0.05, **P < 0.01, ***P < 0.001, ****P < 0.0001.

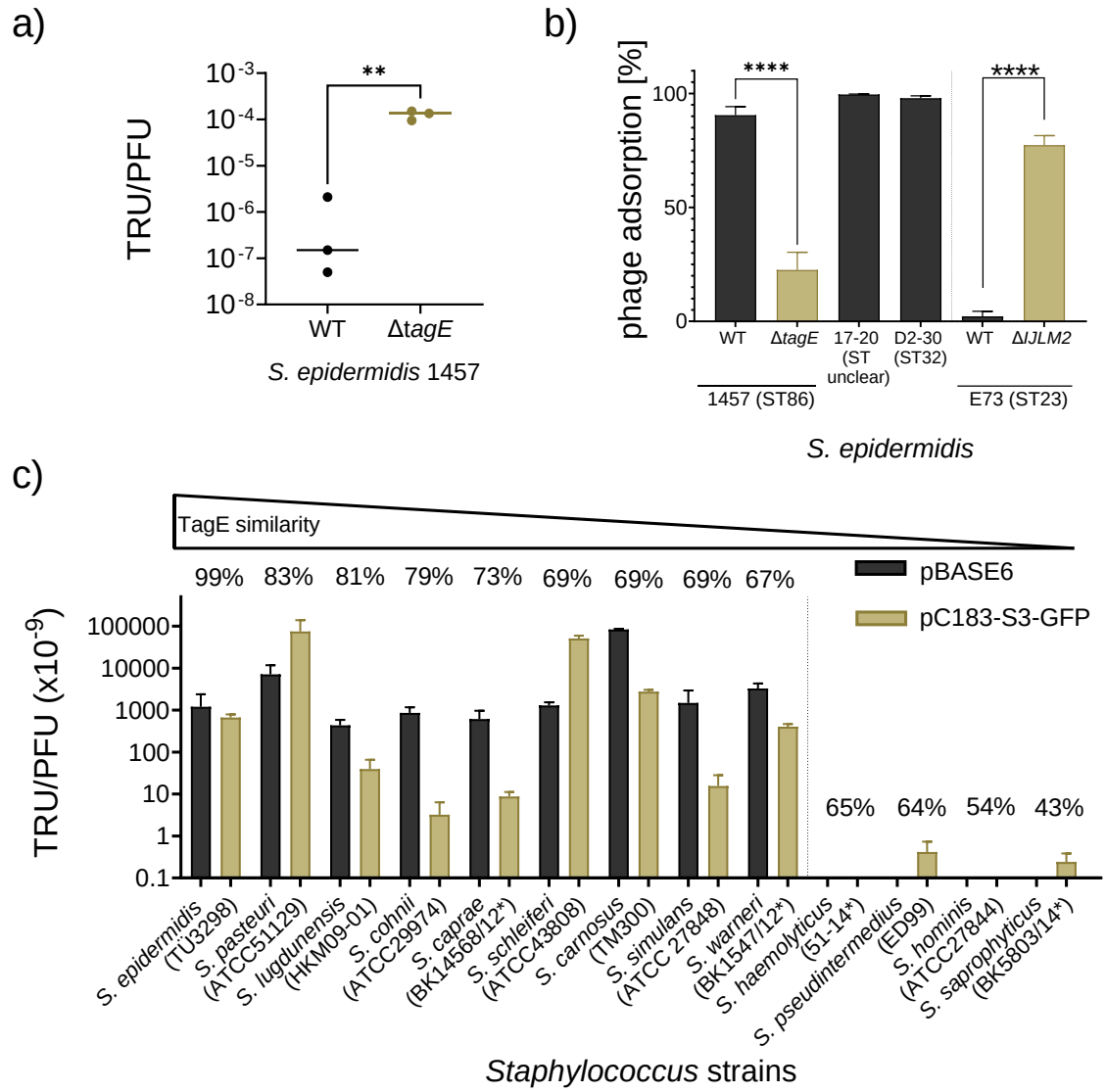

Figure 6: Correlation of TagE-related genes of CoNS species with phage transduction. a) Φ187 transduction of pRB473 is increased in the absence of glucosylated GroP-WTA. b) ΦE72 binds to different strains of *S. epidermidis* but binding is prevented by RboP expression of strain E73. c) ΦE72-mediated transduction of pBASE6 or pC183-S3-GFP to CoNS depends on high TagE homology. If type strains were used to determine sequence similarity of TagE homologues, strain names are marked with an asterisk. The data represents the mean ± SEM of at least three independent experiments. For a,b) unpaired t-test was used to determine statistical significance versus *S. epidermidis* 1457 wild type (WT), indicated as: **P < 0.01, ****P < 0.0001.

623 **Table 1:** Conservation of TagE homologs in CoNS strains used for transduction.

Species	Strain name	Query cover [%]	Sequence identity [%]	Sequence similarity [%]	*tagE*, *pgcA*, *gtaB* encoded together
Staphylococcus epidermidis	TÜ3298	100%	99%	**99%**	Yes
Staphylococcus epidermidis	D2-30	100%	99%	**99%**	Yes
Staphylococcus pasteuri	ATCC51129	100%	69%	**83%**	Yes
Staphylococcus lugdunensis	HKU09-01	99%	64%	**81%**	Yes
Staphylococcus cohnii	ATCC29974	99%	61%	**79%**	No
Staphylococcus caprae	ATCC35538	100%	52%	**73%**	No
Staphylococcus schleiferi	ATCC43808	98%	50%	**69%**	No
Staphylococcus carnosus	TM300	99%	48%	**69%**	No
Staphylococcus simulans	ATCC27848	99%	46%	**69%**	No
Staphylococcus warneri	ATCC27836	99%	47%	**67%**	No
Staphylococcus haemolyticus	ATCC29970	99%	45%	**65%**	No
Staphylococcus pseudointermedius	ED99	100%	43%	**64%**	No
Staphylococcus hominis	ATCC27844	65%	28%	**54%**	No
Staphylococcus saprophyticus	ATCC15305	85%	24%	**43%**	No

624

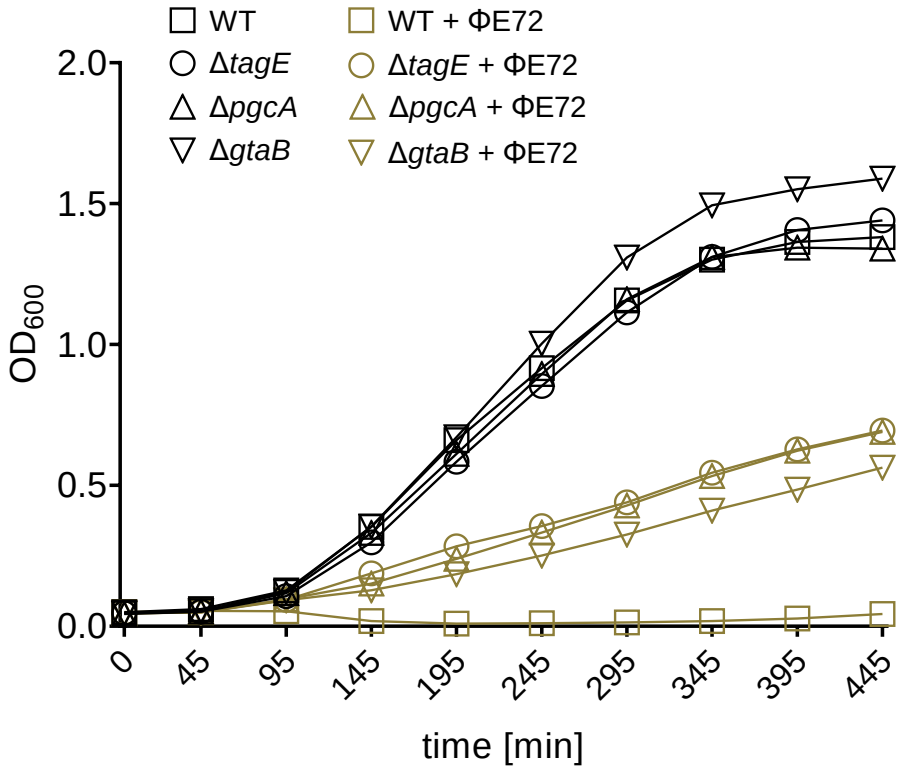

Fig. S1: ΦE72 prevents growth of *S. epidermidis* 1457 wild type (WT). Growth of the Δ*tagE*, Δ*pgcA,* Δ*gtaB* mutants is only partially reduced by ΦE72 compared to growth without addition of phage. Approximately 5x10^8 PFU/ml were used. Data represent mean ± SEM of three independent experiments.

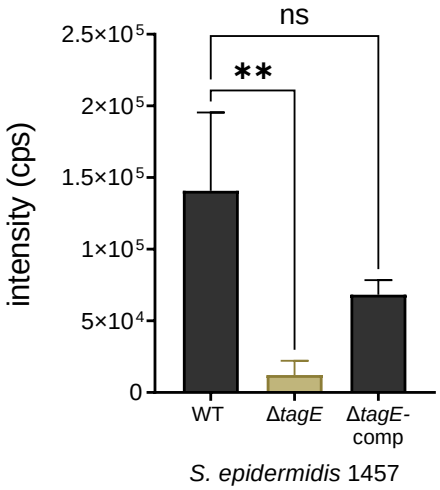

Fig. S2: Area-under-the-curve quantification of GroP-GroP-Glc residue ([M - H]$^-$ = 487.0623) total ion current (TIC) chromatogram measured by HPLC-MS after chemical digest of *S. epidermidis* WTA. Data represent mean ± SEM of three independent experiments. Ordinary one-way ANOVA was used to determine statistical significance versus *S. epidermidis* 1457 wild type (WT), indicated as: not significant (ns), **P < 0.01.

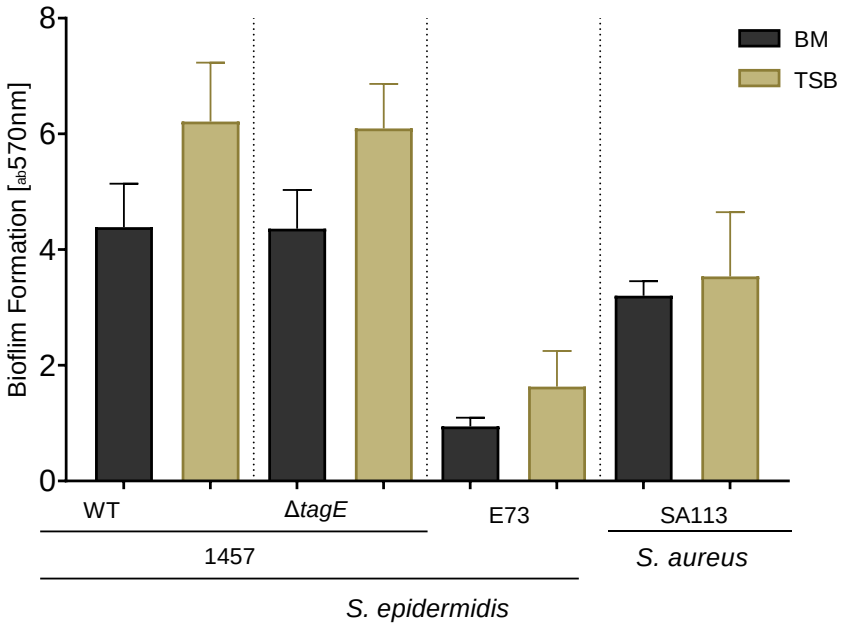

636

637 **Fig. S3:** *S. epidermidis* 1457 biofilm formation was measured in BM and TSB medium. Biofilm formation
638 is unchanged in the Δ*tagE* deletion mutant.

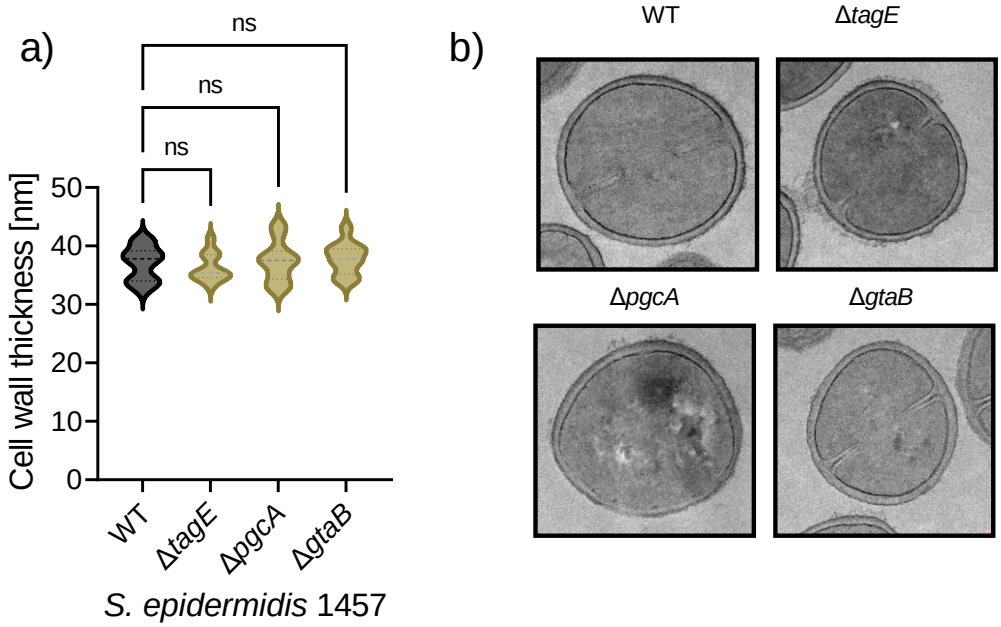

639

640 **Fig. S4:** Electron microscopy at 12,500 x magnification indicates that cell wall thickness (a), and cell
641 shape (b), is unchanged in all mutants compared to the wild type. a) shows the mean cell wall thickness
642 of at least 11 different bacterial cells of each mutant or the wild type (WT). Ordinary one-way ANOVA
643 was used to determine statistical significance versus *S. epidermidis* 1457 wild type (WT), indicated as:
644 not significant (ns).

645

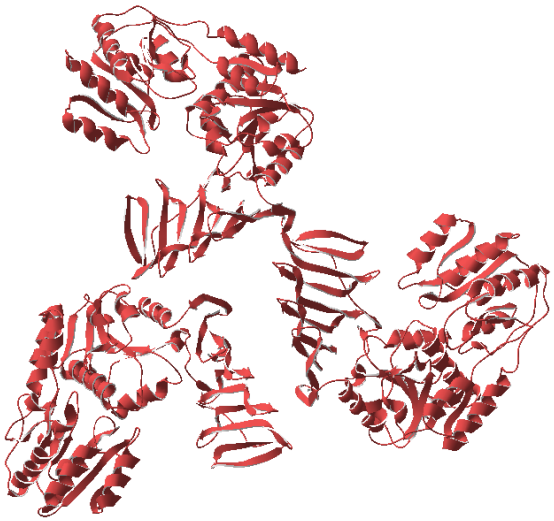

Fig. S5: Structural prediction of the *S. epidermidis* TagE trimer with Alphafold2 [44, 45].

Table S1: Bacteriophages and bacterial strains used in this study.

Bacteriophage	Propagation strain	Morphology	Reference or origin
ΦE72	*S. epidermidis* 1457	siphovirus	Fišarová et al
Φ459	*S. epidermidis* SE459	siphovirus	Fišarová et al
Φ456	*S. epidermidis* SE456	siphovirus	Fišarová et al
Φ27	*S. epidermidis* SE27	siphovirus	Fišarová et al
Φ15	*S. epidermidis* SE15	siphovirus	Fišarová et al
Φ187	*S. aureus* PS187	siphovirus	Pantůcek et al
ΦUKE3	*S. epidermidis* DSM18857	podovirus	DSMZ*
ΦSpree	*S. epidermidis* DSM18857	podovirus	DSMZ*
ΦBE03	*S. epidermidis* SKNA73	podovirus	Valente et al.**
ΦBVG	*S. epidermidis* DSM20608	podovirus	DSMZ*
ΦPauli	*S. epidermidis* DSM20608	podovirus	DSMZ*
ΦNepomuk	*S. epidermidis* DSM20044	podovirus	DSMZ*
ΦBE04	*S. epidermidis* SKNA34	myovirus	Valente et al.**
ΦBE06	*S. epidermidis* SKNA34	myovirus	Valente et al.**
ΦAlex	*S. epidermidis* DSM3269	myovirus	DSMZ*
ΦK	*S. epidermidis* RN4220	myovirus	O'Flaherty et al.

* DSMZ: German Collection of Microorganisms and Cell Cultures

** Department of Intensive Care Medicine, Inselspital, Bern University Hospital, Switzerland

653 **Table S2:** Primer sequences used for cloning and sequencing.

Primer name	Primer sequence	Application
tagE F1-For	ATCTGAATTCAGTAAATCAGCATCAATAAG	Deletion of *S. epidermidis tagE*
tagE F1-Rev	TTTGAGATCTGAAATTTTATAATGTGATTTAAGAAG	Deletion of *S. epidermidis tagE*
tagE F2-For	TATAAGATCTTAGGTATTCAGATGGTTTAGATGATC	Deletion of *S. epidermidis tagE*
tagE F2-Rev	ATTAGTCGACAATGCATTAGAAGTTAAATTCGAAC	Deletion of *S. epidermidis tagE*
pgcA F1-For	AAGGGAATTCCAAAAGAAATGTTACCAATATTAG	Deletion of *S. epidermidis pgcA*
pgcA F1-Rev	TTTGAGATCTTAATATCGAAATAGAATTAACATG	Deletion of *S. epidermidis pgcA*
pgcA F2-For	TACGAGATCTTTCGAAAACATAAAAAGTTCTTAG	Deletion of *S. epidermidis pgcA*
pgcA F2-Rev	TTTTGTCGACTTGAATGAAATCTAATTCATTTGC	Deletion of *S. epidermidis pgcA*
gtaB F1-For	GTCTTGGAATTCTAATACCACTCGTATTTACAG	Deletion of *S. epidermidis gtaB*
gtaB F1-Rev	ATATAAGATCTACAGACATCCACTGAAAAACACTAG	Deletion of *S. epidermidis gtaB*
gtaB F2-For	GTCAAGATCTTTTGATTATTAGAAAGGATAGTACCC	Deletion of *S. epidermidis gtaB*
gtaB F2-Rev	TATCTGTCGACAACTTTAATCAATTTGAGTTAGTTG	Deletion of *S. epidermidis gtaB*
TagE Locus Comp-For	TCATGGTACCTTACTTTACTCTCTCAAACAAC	Fragment synthesis for complementation of gene locus containing *tagE*, *pgcA,* and *gtaB*
TagE Locus Comp-Rev	TTCTGTCGACATTCTTGATTAAGTTAATGTTAATATTG	Fragment synthesis for complementation of gene locus containing *tagE*, *pgcA,* and *gtaB*
473 Eco	CCTCAAGCTAGAGAGTCATTACCCC	sequencing of pRB473 and pBASE shuttle vectors
473 Hind	CTGGATTTGTTCAGAACGCTCGG	sequencing of pRB473 shuttle vector
pBASE Hind	CTACTTCTTTCAAACTCTCTCTACG	sequencing of pBase shuttle vector
erm-For	CTATTATTTAACGGGAGGAAA	Sequencing from erythromycin cassette forward
erm-Rev	TAATCTAACGTATTTATCTGCGTA	Sequencing from erythromycin cassette reverse

654

Extended descriptions of detailed methods

WTA compositional analysis

HPLC-MS

Analysis of the WTA polymer composition was performed using an LTQ Orbitrap Velos mass spectrometer (Thermo Fisher Scientific), connected to an ACQUITY ultra-performance liquid chromatography (UPLC) system (Waters Corporation). Separation in the UPLC was carried out using a Phenomenex C18-Gemini® column (150 × 2 mm, 3 µm, 110 Å, Phenomenex) at 37°C with 0.1% formic acid and 0.05% HCO_2NH_4 (A) and CH_3CN (B) buffer system. A single run (injection volume of 5 µl) was performed with a flow rate of 0.2 ml/min and a two-step gradient: after 2.5 min of equilibration with 100% A, a 1-min gradient up to 5% B was followed by a 4-min gradient up to 70% B. After 2 min at 70% B, a re-equilibration step of 2.5 min followed with a flow rate of 4 ml/min. LC-MS data processing was done with UmetaFlow GUI ([56], https://github.com/axelwalter/streamlit-metabolomics-statistics) via extracted ion chromatograms with a mass tolerance of 10 ppm.

NMR

1H NMR spectra were recorded for both, wild-type and Δ*tagE S. epidermidis* strains, and they were carried out on a Bruker DRX-600 spectrometer equipped with a cryo-probe, at 298 K. Chemical shifts of spectra recorded in D_2O were calculated in ppm relative to internal acetone (2.225 and 31.45 ppm). 2D NMR spectra were acquired for *S. epidermidis* wild type only, the spectral width was set to 12 ppm and the frequency carrier placed at the residual HOD peak, suppressed by pre-saturation. Two-dimensional spectra (DQ-COSY, TOCSY, NOESY, gHSQC, and gHMBC) were measured using standard Bruker software. For all experiments, 512 FIDs of 2,048 complex data points were collected, 32 scans per FID were acquired for homonuclear spectra, and 100 and 200 ms of mixing time was used for the TOCSY and NOESY spectra, respectively. Heteronuclear ^{1}H-^{13}C spectra were measured in the ^{1}H-detected mode, gHSQC spectrum was acquired with 40 scans per FID, the GARP sequence was used for ^{13}C decoupling during acquisition; gHMBC scans doubled those of gHSQC spectrum. During processing, each data matrix was zero-filled in both dimensions to give a matrix of 4K × 2K points and was resolution-enhanced in both dimensions by a cosine-bell function before Fourier transformation; data processing and analysis were performed with the Bruker Topspin 3 program.

NMR analysis of the WTA of the wild type (WT) strain of *Staphylococcus epidermidis*

NMR analyses of the spectra displayed several signals in the anomeric region (5.5 – 4.4 ppm, Fig. 3c) of the proton spectrum with the one at 5.20 ppm being more intense than the others. Then, inspection of the HSQC spectrum (Fig S6a) disclosed that only the signals at ~ 5.2 and ~ 5.1 ppm arose by the anomeric position of different monosaccharide residues, due to the characteristic values of the related carbon atoms (Table S3, [57]). The full assignment of both proton and carbon chemical shifts was possible with confidence only for the most abundant unit, labelled with **A.** Thus, the anomeric proton at 5.2 ppm was labelled $\mathbf{A_1}$, and the combined analysis of the TOCSY and COSY spectra determined that it was an α-glucose (Fig. S6b). Indeed, the TOCSY spectrum showed that $\mathbf{A_1}$ correlated to four other protons as occurs for *gluco* configured residues, and this information combined with those from the COSY spectrum enabled the sequence assignment from H-2 to H-5 (Fig. S6b, Table S3). Then, the identification of A6 was inferred by the finding of the H-4/H-6 cross peak in the TOCSY spectrum (Fig. S6b) while the position of the other H-6 proton, labelled A6' was determined by the strong cross-peak in the COSY spectrum (Fig. S6b). Finally, the identification of the carbon chemical shifts was inferred by analysing the ^{1}H-^{13}C HSQC (Fig. S6a), which determined that **A** was a glucose unit that was not further substituted due to the similarity of its carbon chemical shifts to those reported for the reference glycoside [57]. The inspection of the HMBC spectrum (not shown) reported a cross peak connecting H-1 of **A** to a carbon at 76.7 ppm in turn correlated to a proton at 4.12 ppm, later assigned to H-2/C-2 of a glycerol (Gro) unit, labelled **b**.

Interestingly, H-1 of **A** was flanked by a second anomeric proton at 5.22 ppm (Fig. S6b, Table S3), labelled as **A'** and presenting a correlation pattern in the TOCSY spectrum very similar to that of **A**, except for the fact that the density analogue to $\mathbf{A_{1,5}}$ was missing while there was a new one relating H-1 to a proton at 4.21 ppm. The identification of the sequence between the protons of this second spin system was aided by the COSY spectrum and the additional signal at 4.21 was assigned to H-5, in turn correlated to the two H-6 protons at 4.66 and 4.44 ppm (Fig. S6b), highly deshielded due to the O-acylation with an Ala residue as inferred by the long range correlation with a carbonyl group at 171.5 ppm (not shown).

Then, the anomeric region reported a proton signal at 5.39 ppm, attached to a carbon at 75.5 ppm with only one additional correlation in the COSY spectrum with a proton at ca. 4.1 ppm, assigned with a hydroxy-methyl carbon at 64.9 ppm in the HSQC spectrum (Figure S6a). The pattern of this unit, labelled **a**, was found to be consistent with that of a Gro unit, phosphorylated at both ends and acylated with an Ala unit at O-2, as described in the WTA polymers containing GroP motifs [42].

Finally, the HSQC spectrum contained three densities at ^{1}H/^{13}C 4.04/70.8, and 4.12/76.7, labelled as $\mathbf{c_2}$, and $\mathbf{b_2}$, respectively, all identified with the aid of the values reported in literature (Table S3). In detail,

c was a glycerol unit not further substituted [42], while **b** had the glucose units (**A** and **A'**) linked to O-2 [58]. Of note, the HSQC spectrum contained other densities not related to the WTA polymer and presumably belonging to other compounds co-purified with it. In some cases, it was possible to recognize some amino acids, but it was never possible to establish the nature of the compound(s) due to the low intensities of the signals or to the lack of the proper correlations in the full set of NMR spectra acquired. The integration of the $\mathbf{A}_{5,1}$ and $\mathbf{A'}_{5,1}$ densities in the TOCSY spectrum (Figure S6b) revealed that about 15% of this monosaccharide was derivatized with an alanine at O-6.

Table S3: NMR chemical shifts. ^{1}H (600MHz) chemical shifts of WTA structural motifs found in *S. epidermidis* wild type. The sample was dissolved in deuterated water (HOD, 550 µl) and measured at 298 K. By convention, C-1 of the glycerol unit is placed at the left of the structural formula, P stands for phosphate.

Residue	motif	1;1' (for Gro)	2	3; 3' (for Gro)	4	5	6; 6'
a	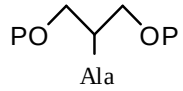	4.11 x 2	5.39	4.11 x 2	--	--	--
Gro		64.9	75.5	64.9	--	--	--
b	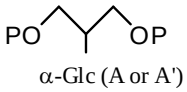	~ 4.02 x 2*	4.12	~ 4.05 – 4.00*	--	--	--
Gro		66.6	76.7	65.8	--	--	--
c		3.85;3.90	4.04	3.85;3.90	--	--	--
Gro		67.5	70.8	67.5	--	--	--
A	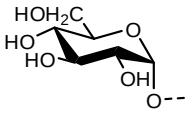	5.20	3.54	3.78	3.41	3.95	3.89; 3.77
t-α-Glc		98.9	72.8	74.3	71.0	73.1	61.9
A'	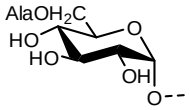	5.22	3.57	3.80	3.43	4.21	4.66; 4.44
t-α-Glc6Ala		96.2	72.6	74.1	71.2	71.0	66.5
Ala	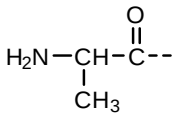	--	4.23	1.62	--	--	--
		171.5	50.1	16.6--	--	--	--

* These signals can be exchanged.

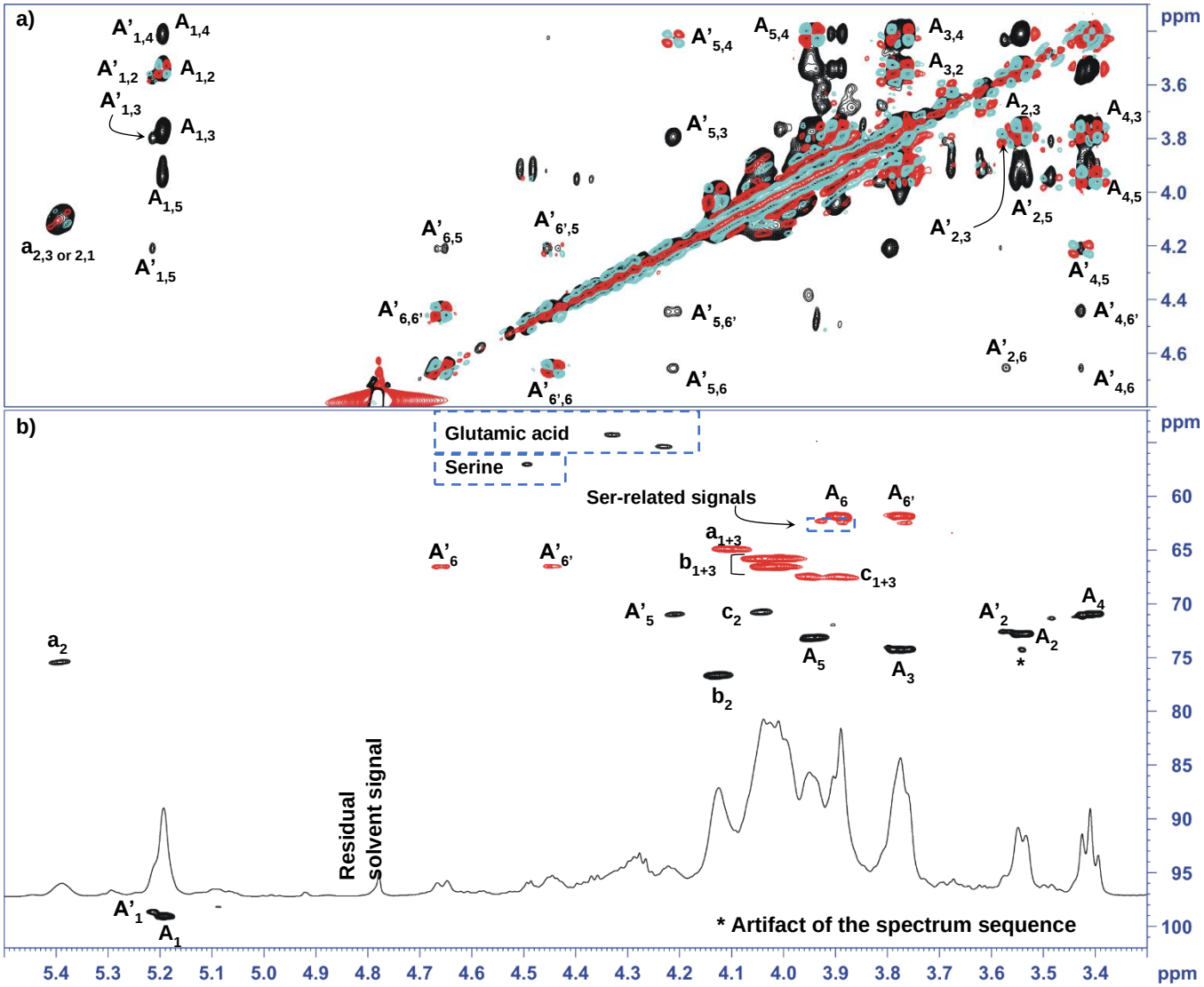

Fig. S6: NMR spectra recorded for WTA isolated from *S. epidermidis* wild type. a) Expansion of the HSQC spectrum detailing the anomeric and the carbinolic region. b) Overlap of the TOCSY (black) and COSY (cyan and red) spectra. In all the spectra, the most relevant densities are labelled with the letter used in Table S3; as for the carbohydrate units (**A** and **A'**), the anomeric signals are indicated with a capital letter, while the Gro units (**a**, **b**, and **c**) are labeled with small letters.